Article published online: 2023-09-12

Diffusion-Weighted Imaging and Chemical Shift Imaging to Differentiate Benign and Malignant Vertebral Lesion: A Hospital-Based Cross-Sectional Study

Kaneez Fatima[1] Suprava Naik[1] Mantu Jain[2] Sanjeev Kumar Bhoi[3] Somnath Padhi[4] Nerbadyswari Deep Bag[1] Ashutosh Panigrahi[5] Sudipta Mohakud[1]

[1] Department of Radiodiagnosis, All India Institute of Medical Sciences, Bhubaneswar, Odisha, India
[2] Department of Orthopaedics, All India Institute of Medical Sciences, Bhubaneswar, Odisha, India
[3] Department of Neurology, All India Institute of Medical Sciences, Bhubaneswar, Odisha, India
[4] Department of Pathology, All India Institute of Medical Sciences, Bhubaneswar, Odisha, India
[5] Department of Haematology, All India Institute of Medical Sciences, Bhubaneswar, Odisha, India

Address for correspondence Suprava Naik, Department of Radiodiagnosis, All India Institute of Medical Sciences, Bhubaneswar 751019, Odisha, India (e-mail: drsuprava.rd@gmail.com).

Indian J Radiol Imaging 2024;34:76–84.

Abstract

Objective The aim of this study was to evaluate the role of diffusion-weighted imaging (DWI) and chemical shift imaging (CSI) for the differentiation of benign and malignant vertebral lesions.

Methods Patients with vertebral lesions underwent routine magnetic resonance imaging (MRI) along with DWI and CSI. Qualitative analysis of the morphological features was done by routine MRI. Quantitative analysis of apparent diffusion coefficient (ADC) from DWI and fat fraction (FF) from CSI was done and compared between benign and malignant vertebral lesions.

Results Seventy-two patients were included. No significant difference was noted in signal intensities of benign and malignant lesions on conventional MRI sequences. Posterior element involvement, paravertebral soft-tissue lesion, and posterior vertebral bulge were common in malignant lesion, whereas epidural/paravertebral collection, absence of posterior vertebral bulge, and multiple compression fractures were common in benign vertebral lesion ($p < 0.001$). The mean ADC value was 1.25 ± 0.27 mm^2/s for benign lesions and 0.9 ± 0.19 mm^2/s for malignant vertebral lesions ($p \leq 0.001$). The mean value of FF was 12.7 ± 7.49 for the benign group and 4.04 ± 2.6 for the malignant group ($p < 0.001$). A receiver operating characteristic (ROC) curve analysis showed that an ADC cutoff of 1.05×10^{-3} mm^2/s and an FF cutoff of 6.9 can differentiate benign from malignant vertebral lesions, with the former having 86% sensitivity and 82.8% specificity and the latter having 93% sensitivity and 96.6% specificity.

Keywords
- diffusion-weighted imaging
- chemical shift imaging
- fat fraction
- Dixon sequence

article published online
September 12, 2023

DOI https://doi.org/10.1055/s-0043-1772848.
ISSN 0971-3026.

Thieme Medical and Scientific Publishers Pvt. Ltd., A-12, 2nd Floor, Sector 2, Noida-201301 UP, India

Conclusion The addition of DWI and CSI to routine MRI protocol in patients with vertebral lesions promises to be very helpful in differentiating benign from malignant vertebral lesions when difficulty in qualitative interpretation of conventional MR images arises.

Introduction

Vertebral lesions in elderly and in patients with known malignancy are quite a common occurrence. It can be due to various etiologies, such as degenerative changes, infections, trauma, and malignancy.[1] The spine is the most frequent site of osseous metastasis in the body. Metastasis from carcinoma breast, kidney, and thyroid is associated with an increased risk of pathological fractures and compressive myelopathy.[2] It is at times difficult to differentiate from benign osteoporotic fracture as a result of decreased bone density, especially in elderly females.[3]

Apart from this, trauma, infective spondylodiskitis, and primary vertebral neoplasm also can present with complications such as vertebral fracture and compressive myelopathy. Hence, it is essential to distinguish malignant and benign vertebral lesions as it affects treatment strategy, clinical staging, and prognosis in patients with proven malignancies.

Although histopathological diagnosis is the gold standard, it is invasive and associated with its own complications. Also, it is sometimes not feasible, especially if the lesion is located in the cervical spine. A positron emission tomography (PET) scan can be useful in some cases; however, it also has its limitations in differentiating malignant and infective lesions as both may show uptake.

Magnetic resonance imaging (MRI) is an excellent noninvasive method for the assessment of bone marrow lesions with high spatial resolution. Apart from gross morphological data, MRI gives information about cellular and chemical levels.[4] Conventional MRI is highly sensitive in detecting abnormality; however, it lacks specificity. It sometimes can represent a diagnostic conundrum, specifically in case of the elderly patients and in patients with known cases of cancer. The sensitivity of T1-weighted (T1W), T2-weighted (T2W) imaging, and short tau inversion recovery (STIR) sequence is quite high, but the specificity of these sequences to discriminate between benign and malignant lesions is low. This is due to the fact that signal alterations seen in bone marrow edema due to benign causes is similar to that observed in bony metastasis.[4]

MRI techniques reflecting distinct aspects of the chemical environment and pathophysiology of vertebral marrow lesions have been put forward to distinguish benign vertebral lesions from malignant vertebral lesions with more accuracy. Diffusion-weighted imaging (DWI) measures the random Brownian motion of water molecules.[5] Studies have shown significantly lower apparent diffusion coefficient (ADC) value in malignant lesions compared with benign lesions.[5,6] There is a paucity of studies in the literature regarding the correlation of the vertebral lesion with the vertebral marrow fat fraction (FF). In this study, we evaluated the role of DWI and vertebral body FF obtained from chemical shift MRI to differentiate between benign and malignant vertebral lesions.

Material and Methods

This is a cross-sectional hospital-based study performed in a tertiary care teaching institute after obtaining ethical clearance from the institutional ethics committee. Patients older than 18 years having vertebral lesions with or without fractures were included. A sample size of 72 was obtained with a confidence interval of 95%. After obtaining informed consent, the enrolled patients underwent MRI in a 3-T MRI scanner (Discovery MR750W, GE Healthcare) using a 32-channel spine coil. The protocol is discussed in the following section.

Magnetic Resonance Imaging Protocol

The following protocols were used: sagittal T2WI (repetition time [TR]/echo time [TE]: 4,474/85 milliseconds, field of view [FOV]: 28.0 cm, number of excitations [NEX]: 3.00); sagittal T1W (TR/TE: 671/13.5 milliseconds, FOV: 28.0 cm, NEX: 2.00); axial T2WI (TR/TE: 4,209/85 milliseconds, FOV: 28 cm, NEX: 3.00, slice thickness: 3.0 mm, interslice distancing: 0.3 mm); sagittal STIR (TR/TE: 4,333/68 milliseconds, FOV: 28 cm, NEX: 2.00, slice thickness of 3 mm, interslice gap of 0.3 mm); sagittal DWI (TR/TE: 3430/69.1 milliseconds, FOV: 24 cm, *b*-value: 50 and 800, slice thickness: 4.0 mm, interslice distancing: 0 mm); and IDEAL-IQ (TR/TE: 8.9/4.0 milliseconds, FOV: 40 cm, NEX: 3, echoes: 6, slice thickness: 4.0 mm, interslice distancing: 0.4 mm). Gadolinium-based intravenous contrast was administered on a case-to-case basis when required, and postcontrast T1WI was acquired in sagittal and axial planes.

Computed Tomography–Guided Biopsy

Computed tomography (CT) guided percutaneous biopsy was done from vertebral lesions as per standard management protocol. Under strict aseptic precaution, percutaneous vertebral biopsy using a Jamshidi bone biopsy needle through the transpedicular/posterolateral extrapedicular technique was performed after administration of adequate amount of local anesthesia. Precaution was taken to avoid injury to exiting nerve roots and great vessels. In the presence of multiple lesions, the largest and most approachable lesion was selected, for example, a lumbar vertebral lesion was preferred over dorsal and cervical vertebral lesions. In patients with associated paravertebral soft-tissue component, both bone and soft-

tissue components were biopsied simultaneously. In patients with associated paravertebral collection, ultrasonography (USG)/CT-guided aspiration was also done as per the feasibility. A sample for microbiological examination was also obtained if an infection was suspected.

In patients with known primary malignancy elsewhere in the body, biopsy was not done if there were multiple vertebral lesions considering the same as metastasis. However, biopsy was done in the solitary indeterminate vertebral lesion in case of known malignancy to guide the clinical staging, treatment planning, and overall prognosis of the patient.

Elderly patients with suspected osteoporotic collapse underwent a dual-energy X-ray absorptiometry (DEXA) scan to measure bone density. A *T*-score of ≤ -2.5 was considered diagnostic of osteoporosis and biopsy was exempted in these cases. Patients with a history of trauma were also exempted from vertebral biopsy.

Reports of all of the above-mentioned investigations were collected. Patients, in whom biopsy/aspiration was not done, were followed up either with imaging or clinically, depending on the etiology. If the lesion appearance remained the same after 6 months of follow-up without progression or the patient improved clinically, the lesion was considered benign.

Data Collection and Image Analysis

MR images were transferred to the Advantage Workstation Server (AWS), GE Healthcare. Two experienced radiologists having more than 12 years' experience analyzed the MR images. In case of interobserver variation, final imaging diagnosis was made by consensus. Imaging findings and qualitative and quantitative MRI parameters were recorded. MRI features were correlated with histopathological diagnosis and also with microbiological or DEXA scan reports and with history and clinical follow-up wherever suitable.

Involvement of vertebral bodies, posterior elements, presence of paravertebral or epidural collection, paravertebral soft-tissue lesion, posterior vertebral bulge, cortical disruption, and presence/absence of fracture were noted. Signal intensity of the involved vertebra was qualitatively analyzed by comparing with that of an uninvolved vertebra, on T1W, T2W, STIR, and DWI sequence.

Quantitative analysis of DWI was done by calculating the ADC value using "READY View" postprocessing application. Regions of interest (ROIs) of varying sizes were drawn over the lesion on DWI that corresponded to signal changes on the T1WI and STIR. Three ROIs were drawn over the lesion and the ADC values were obtained. The mean ADC was calculated by averaging them. The ADC values were also obtained from the adjacent normal vertebrae by drawing the ROIs.

The ROI was dependent on the size of the lesion in focal discrete lesions, but in the cases where there was diffuse vertebral marrow involvement, it was drawn as large as possible placed in the antero-central aspect of the vertebral body avoiding the basivertebral venous plexus and endplate degenerative changes. The ROIs varied between 10 and 60 mm^2 in each lesion.

FF was obtained from the Iterative Decomposition of water and fat with Echo Asymmetry and Least squares estimation Quantitation (IDEAL-IQ) sequence that is a modified multi-echo Dixon technique. ROIs as placed on DWI were also placed in a similar way in the FF image. Normalized FF was computed by dividing the FF of the involved vertebrae by the FF of the normal-appearing vertebra.

The final diagnosis that was made on the basis of biopsy results or results of at least 6 months of clinical or radiological follow-up. This was used as the "gold standard" to classify the vertebral lesion as benign or malignant.

Statistical Analysis

All the statistical analyses were done using IBM SPSS 29.0 version. Continuous variables were summarized in the form of means and standard deviation (SD) and categorical variables were expressed as frequencies and percentages. Nonparametric variables between two groups were compared using the Mann–Whitney *U* test. The correlation between two nonparametric variables wase assessed using Spearman's rank correlation coefficient. The chi-squared test was applied for comparing categorical variables between benign and malignant groups. Receiver operating characteristics (ROC) curve analysis was used to find out the cutoff value for ADC, FF, and normalized FF to determine the optimal cutoff.

The diagnostic value of diffusion restriction was examined by two-by-two contingency tables with the ultimate classification of lesions into two broad categories, that is, benign and malignant. The sensitivity and specificity were then calculated.

For all the statistical tests used, the level of significance was set at a *p*-Value less than 0.05.

Results

A total of 72 patients were included in our study. Out of the total patients enrolled, 39 (45.8%) were males. Details of the demographic findings are given in ►**Table 1**. Out of 72 patients, 43 cases were benign and 29 were malignant as per the final diagnosis. CT-guided biopsy was done in 56 patients (out of which 34 turned out to be benign and 22 malignant). The most common presenting complain was back pain in 62 patients [86.1%], followed by lower limb weakness in 6 (8.3%) and inability to walk in 4 (5.6%) patients. Twenty-one of 72 (29.2%) patients showed solitary vertebral lesions; the remaining 51 (70.8%) patients showed multiple vertebral involvements. Eighty-two vertebrae were involved in the benign category, whereas 63 vertebrae were involved in the malignant category.

Twenty-five of 43 patients in the benign category were of tubercular etiology. Other benign causes of vertebral lesions included pyogenic spondylosis ($n=9$), traumatic vertebral fracture ($n=5$), and osteoporotic vertebral collapse ($n=4$). The most common malignant cause included metastasis ($n=12$), followed by multiple myeloma ($n=12$), plasmacytoma ($n=3$), Ewing's sarcoma ($n=1$), and giant cell tumor ($n=1$; ►**Table 2**). Out of 12 patients of vertebral metastasis, 7

Table 1 Clinical and demography of the patients in the study ($n = 72$)

Characteristics		Benign ($n = 43$)	Malignant ($n = 29$)
Mean age (y), mean ± SD (range)		46.86 ± 14.22 (18–82)	52.55 ± 13.33 (18–83)
Duration of symptoms (d), mean ± SD (range)		42.16 ± 26.76 (2–90)	37 ± 26.35 (10–90)
Sex	Male	24	15
	Female	19	14
No. of lesions (%)		82 (56.6)	63 (43.4)

Abbreviation: SD, standard deviation.

Table 2 MRI findings in benign and malignant vertebral lesions

Parameters	Benign ($n = 43$), number (%)	Malignant ($n = 29$), number (%)	*p*-Value
Hypointensity on T1WI	42 (97.7)	29 (100)	0.71
Hyperintensity on T2WI	42 (97.7)	28 (96.6)	0.54
Hyperintensity STIR	43 (100)	29 (100)	1
Posterior element involvement	24 (55.8)	28 (96.6)	<0.001
Epidural/paravertebral collection	30 (69.8)	0 (0)	<0.001
Paravertebral soft-tissue lesion	1 (3.8)	25 (96.2)	<0.001
Diffusion restriction	5 (11.6)	26 (89.7)	<0.001
Posterior vertebral bulge	1 (2.3)	22 (75.9)	<0.001
Intervertebral disk space involvement	26 (60.5)	0 (0)	<0.001
Fracture present	24 (55.8)	10 (34.5)	0.075

Abbreviations: MRI, magnetic resonance imaging; STIR, short tau inversion recovery; T1WI, T1-weighted imaging; T2WI, T2-weighted imaging.

patients had lung carcinoma, 3 had breast carcinoma, and 2 had stomach carcinoma. Diagnosis of the same was confirmed from biopsy from the primary site.

In our study, all the vertebrae in the malignant category ($n = 29$) and 42 (97.7%) vertebrae in the benign category showed hypointense signal on T1WI. One vertebra in the benign category was isointense on T1W imaging in comparison with normal marrow.

On T2WI, 42 of 43 vertebrae in benign group were hyperintense; one case of sclerotic metastasis was hypointense. In the benign group ($n = 29$), 28 were hyperintense on T2WI and 1 was isointense. All the involved vertebrae, whether benign or malignant, were hyperintense on STIR sequence.

The signal intensity of conventional MRI sequences was not statistically significant in distinguishing between neoplastic and non-neoplastic lesions. However, some additional findings like involvement of posterior elements and presence of paravertebral soft tissue or abscess were significant between the two groups. Details of the MRI findings are given in ►**Table 2**.

We could not find a significant correlation between the ADC values of normal-appearing vertebra and age (Spearman's correlation coefficient: –0.04; $p = 0.72$). However, a weak but significant positive correlation was found between the FF values of normal vertebrae and age (Spearman's correlation coefficient: 0.3; $p = 0.009$).

Diffusion restriction was noted more commonly in the malignant lesion. FF was reduced in both benign and malignant lesions although to a greater degree in malignant lesions (►**Figs. 1** and **2**). The mean ADC value for benign lesion ($1.25 \pm 0.27 \times 10^{-3}$ mm^2/s) was significantly higher than that of malignant lesion ($0.88 \pm 0.19 \times 10^{-3}$ mm^2/s; $p = 0.001$). The ROC curve shows an ADC cutoff of 1.05×10^{-3} mm^2/s can differentiate between benign and malignant vertebral lesion with 86% sensitivity and 82.8% specificity, and area under the curve (AUC) of 0.9 (►**Fig. 3**).

The mean FF of vertebral lesions in the benign group was 12.7 ± 7.49, which was significantly higher than that of the malignant group (4.04 ± 2.6; $p = 0.001$). The ROC curve for FF shows an AUC of 0.95. Considering a cutoff value of FF of 6.9, benign vertebral lesions can be differentiated from malignant lesions with a 93% sensitivity and 96.6% specificity (►**Fig. 3**).

The mean normalized FF (FF of the vertebral lesion divided by normal-appearing noncontiguous vertebra) of vertebral lesions in the benign group was 0.37 ± 0.24, which was significantly higher than that of the malignant group (0.1 ± 0.06; $p = 0.001$). The ROC curve for normalized FF shows an AUC of 0.954. Considering a cutoff value of normalized FF of 0.17, benign and malignant vertebral lesions can be differentiated with a 90.7% sensitivity and 89.7% specificity (►**Fig. 3**). Details of the ADC and FF are been given in ►**Table 3**.

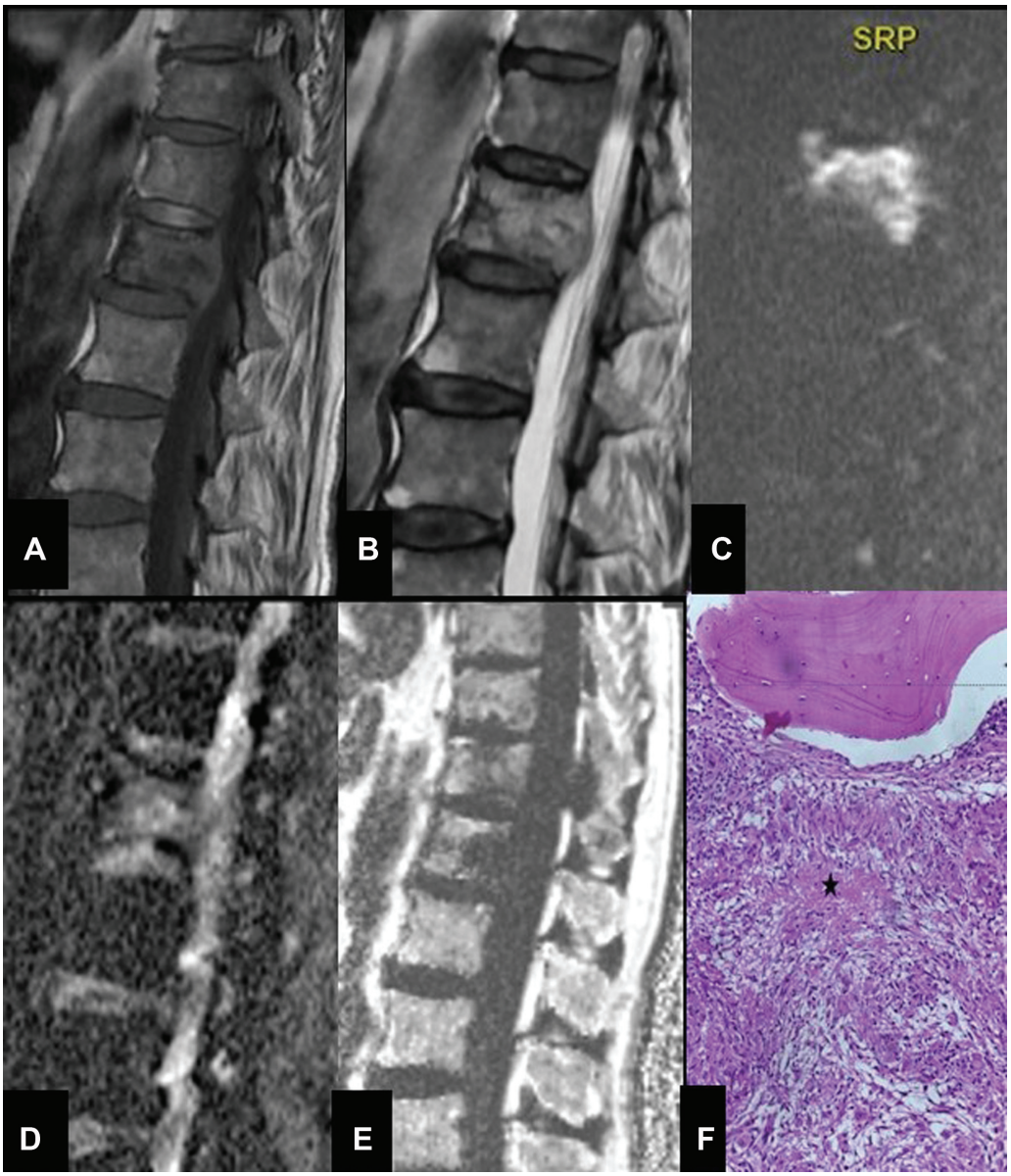

Fig. 1 Magnetic resonance imaging (MRI) of dorsal spine in a 65-year-old man with D11 vertebral lesion. (**A**) Sagittal T1-weighted imaging (T1WI) and (**B**) T2-weighted imaging (T2WI) show T1 hypointense and T2 hyperintense lesion involving the D11 vertebra with posterior bulge of the vertebra. The lesion appears hyperintense on (**C**) diffusion-weighted imaging (DWI) as well as on (**D**) apparent diffusion coefficient (ADC) map suggesting T2 shine through. (**E**) Fat fraction (FF) of the lesion was 8.1%. (**F**) Histopathology shows well-formed, coalescent, epithelioid granulomas comprising multifocal localized collections of epithelioid histiocytes admixed with small mature lymphocytes (hematoxylin and eosin, ×200,) and patchy areas of central caseous necrosis (*black asterisk*), suggestive of mycobacterial etiology.

Discussion

This study describes the imaging findings of vertebral lesions in 72 patients and the role of DWI and chemical shift imaging in distinguishing between benign and malignant vertebral lesions.

Distinguishing benign from malignant vertebral lesions is often a clinical dilemma. The limitations of modalities like plain X-ray, bone scan, CT scan, and MRI in diagnosing benign and malignant lesions have been reported.[7] Bone scintigraphy has high sensitivity but low specificity. Fluorodeoxyglucose-PET (FDG-PET) may distinguish between osteoporotic fractures and malignant fractures; however, it cannot distinguish the inflammatory process from a malignancy as it shows high uptake in both. Another disadvantage is that it exposes patients to ionizing radiation and hence is not recommended in young patients.[8]

MRI is a noninvasive imaging modality that is often used to study the signal intensity of bone marrow as well as the complications like vertebral fracture and compressive myelopathy. On routine MRI, vertebral lesions are usually seen as T1 hypointense signal and T2 hyperintense signal. STIR is even more sensitive in the detection of vertebral lesion because the fat signal of the vertebral marrow is suppressed and even slightest increase in water content stands out prominently.[2] The majority of cases in our study showed

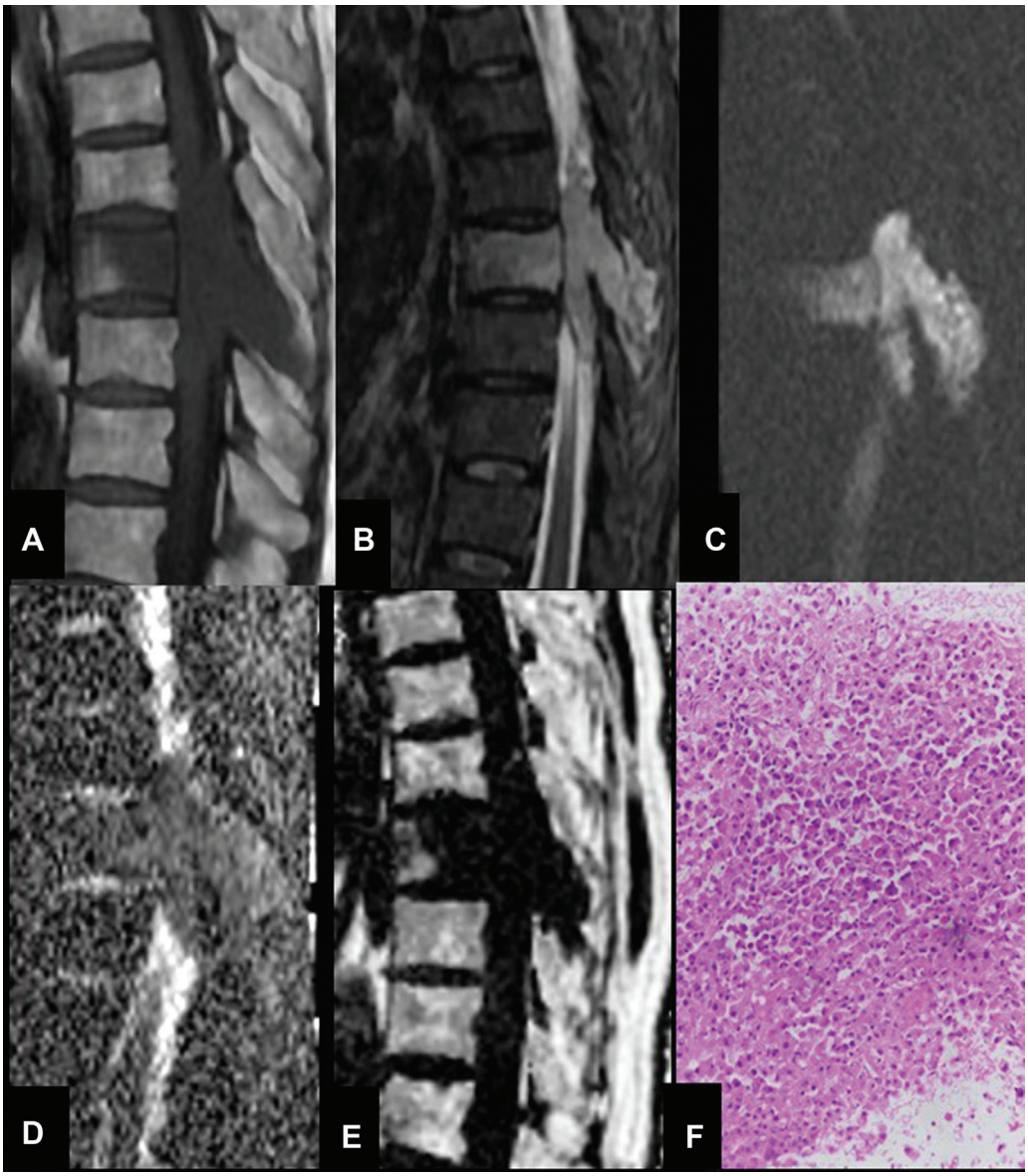

Fig. 2 Spinal magnetic resonance imaging (MRI) of a 38-year-old woman with a biopsy-proven plasmacytoma involving the D9 vertebra. (**A**) Sagittal T1-weighted imaging (T1WI), (**B**) T2-weighted imaging (T2WI) show T1 hypointense, T2 hyperintense, lesion involving the body and posterior element of the D9 vertebra with an epidural component causing cord compression. The lesion appears hyperintense on diffusion-weighted imaging (DWI) (**C**) and hypointense on corresponding apparent diffusion coefficient (ADC) map. (**D**) The ADC value was 0.77×10^{-3} mm^2/s. (**E**) The fat fraction (FF) of the lesion was 3.1%. (**F**) Histopathology, Hematoxylin eosin, × 200 shows cellular lesion comprising of plasma cells with eccentrically placed nuclei showing moderate atypia.

T1 hypointensity and T2/STIR hyperintensity. Although MRI is highly sensitive in detecting marrow changes, it lacks specificity because the conventional MRI sequences show similar signal intensity in both benign and malignant vertebral lesions.[9,10]

Some of the coexisting findings may help in narrowing the differentials of a vertebral lesion. Involvement of the posterior elements is common in metastasis; however, spinal tuberculosis often affects the posterior elements of the vertebrae along with the body and intervertebral disk. Isolated involvement of the posterior elements is rare in tuberculosis. A combination of paravertebral collection and posterior element involvement was found in infective lesions. Involvement of the posterior element along with a paravertebral soft-tissue lesion is commonly seen in malignant vertebral lesions.[11] At times, organized collection or granulation tissue may mimic paravertebral soft tissue. Intervertebral disk space is commonly involved in infective lesions, more so in pyogenic spondylodiskitis and also in the later stage of tuberculosis. Intervertebral disk space is almost never involved in metastasis. Many times, a diagnostic dilemma exists, especially when there is isolated vertebral involvement without involvement of the intervertebral disk or the paraspinal and epidural soft tissue or abscesses.

Macroscopic information obtained by routine sequences can be supplemented by DWI, which gives information about tissue organization at the microscopic level. Brownian motion of water molecules is affected due to pathological changes in

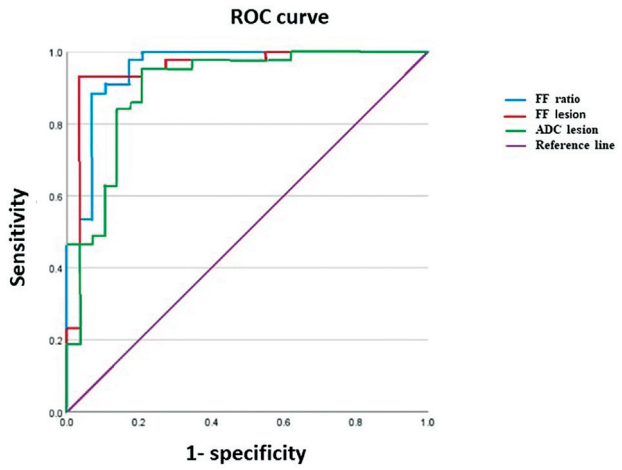

Fig. 3 Receiver operating characteristic (ROC) curve showing sensitivity and specificity of apparent diffusion coefficient (ADC), fat fraction (FF), and normalized FF in differentiating between benign and malignant vertebral lesions.

tissue, which alter the signal intensity. In cases of neoplastic pathologies, there is high cellularity with increased nucleus-to-cytoplasmic ratio, which causes inhibition of movement of water molecules resulting in restricted diffusion that is seen as hyperintense signal on DWI and hypointense signal on ADC map. However, in cases of benign pathologies, there is comparatively free diffusion due to abundance of cytoplasm, loose arrangement of cells and more free water content.[12] The value of DWI in spine imaging has been successfully implied in various clinical situations.[13,14]

Several studies have analyzed DWI qualitatively for neoplastic and non-neoplastic vertebral lesions.[15] However, visual assessment of hyperintensity on DWI lacks specificity as it can also be caused by active hematopoietic red marrow and inflammation. Quantitative analysis of DWI through measurement of ADC has been tried by many authors.[15–17] The importance of ADC is that the T2 effect from diffusion images is eliminated and a quantifiable signal is obtained, which is directly proportional to the degree of Brownian motion of water molecules.[18]

Sheikh et al[19] reported a mean ADC value of $0.81 \pm 0.19\,mm^2/s$ for malignant lesions and $1.2 \pm 0.24\,mm^2/s$ for benign lesions. This is akin to many previous studies that showed higher ADC measurements in benign vertebral lesions compared with malignant vertebral lesions.[18,20,21] We also found a significantly higher mean ADC value in benign lesions compared with malignant lesions ($p < 0.001$). The results of our study are also in congruence with Allam et al who reported 85.7% sensitivity and 91.3% specificity with a cutoff value of $0.9 \times 10^{-3}\,mm^2/s$.[22] Contrary to this, Turna et al reported that ADC measurements were not helpful in differentiating neoplastic from non-neoplastic vertebral lesions and there was considerable overlapping in the two groups.[23] This disparity might have arisen due to the size and placement of ROI and variations in the technique and acquisition of MRI. This could also be due to different stages of the pathological conditions affecting the vertebrae.

Lavdas et al[24] reported ADC varies significantly with age; however, we could not find any significant correlation of ADC of vertebral marrow with age. It may be due to the exclusion of patients younger than 18 years. Also, many patients were middle-aged (interquartile range: 39–59.75 years). Another cause could be that the normal-appearing vertebra in some cases as in infiltrative diseases like multiple myeloma may not actually be normal.

The fundamental basis of chemical shift MRI is that hydrogen protons in water and fat precess slightly differently. At 3 T, fat and water protons are in phase with each other at TE of 2.24 milliseconds and out of phase at TE of 1.12 milliseconds. This results in cyclical addition (in phase) and cancellation (out of phase) of signal intensities of water and fat. So the presence of both water and fat molecules in a single voxel results in signal drop on opposed phase imaging. The advantages of CSI include a short acquisition time, high signal-to-noise ratio and no contrast administration.

IDEAL-IQ is a newer fat–water separation method based on chemical shift imaging for assessing bone marrow FF. IDEAL-IQ is a rapid and highly reproducible method to separate fat and water.[25] It is a method that uses the six-echo Dixon method to quantify FF by correcting all the confounding factors like inhomogeneity effects of the main magnetic field, $T2^*$ effects, multiple peaks in fat spectrum, T1 effects, and eddy currents, which affect dual-echo chemical shift-encoded imaging.[26]

Estimation of FF from these methods should improve the diagnostic performance of chemical-shift MRI in differentiating neoplastic and non-neoplastic lesions.

Table 3 Quantitative diffusion and CSI parameters of the benign and malignant vertebral lesions

Parameters	Benign ($n = 43$), mean ± SD (range)	Malignant ($n = 29$), mean ± SD (range)	*p*-Value
ADC	1.25 ± 0.27 (0.84–2.61)	0.88 ± 0.19 (0.56–1.53)	<0.001
Normalized ADC ADC vertebral lesion/ADC normal-appearing vertebra	2.57 ± 0.78 (1.6–5.6)	2.02 ± 1.16 (1.16–7.5)	<0.001
Fat Fraction (%)	12.7 ± 7.49 (3.4 ± 39.7)	4.04 ± 2.6 (0.22–13.8)	<0.001
Normalized FF (FF involved vertebra/FF normal-appearing vertebra)	0.37 ± 0.24 (0.12- 1.2)	0.1 ± 0.06 (0.0–0.3)	<0.001

Abbreviations: ADC, apparent diffusion coefficient; CSI, chemical shift imaging; FF, fat fraction; SD, standard deviation.

Kim et al[27] investigated the feasibility of FF in differentiating malignant marrow-replacing lesions from benign red marrow deposition with a T2*-corrected FF map using a 3D volume interpolated breath-hold gradient echo Dixon sequence. They observed that FF and normalized FF can be used to differentiate benign vertebral lesions from malignant vertebral lesions with sensitivity of 85.7% and specificity of 100%. FF at a cutoff of 5.26% had high diagnostic performance (AUC: 0.98). In another study, Yoo et al[26] reported the cutoff of 6.34 with 95% sensitivity and 95% specificity for distinguishing between benign and malignant lesions. These are in agreement with our study, where the mean value of FF in the benign group was significantly higher than that of the malignant group allowing differentiation between two types of lesions.

We found a weak positive correlation between the FF of normal vertebrae and age. The FF of the vertebra increases significantly with increasing age.[28,29]

The ADC value, FF, and normalized FF can adequately distinguish benign vertebral lesions from malignant ones.

The strength of our study is a good sample size and the fact that definitive diagnosis was obtained in most of the cases. However, our study has few limitations. First, lack of histopathological diagnosis in few cases for ethical reasons. Patients with prior definitive diagnosis of primary malignancy elsewhere in the body, history of trauma, and osteoporosis confirmed on DEXA scan were exempted from undergoing biopsy. Second, although we were careful to draw the ROI that best represented the lesion, the readers made a subjective decision on the area of the ROI and the outer margins of the lesion. Third, no subgroup analysis was done in patients with various benign and malignant etiologies.

Conclusion

We conclude that conventional MRI with STIR sequence is highly sensitive in the detection of vertebral lesions; however, it cannot differentiate between a benign and a malignant vertebral lesion. Certain features such as posterior element involvement, paravertebral soft tissue, and collection may help in characterizing a lesion. Advanced imaging modalities like DWI and CSI can be helpful in distinguishing between benign and malignant vertebral lesions with more accuracy and can be added to the routine imaging protocol while dealing with focal or diffuse vertebral lesions.

Informed Consent

Informed consent was obtained from all the participants or their relatives for being included in the study.

Author Contributions

K.F. contributed to data collection, data analysis, literature search, manuscript writing, and manuscript editing. S.N. contributed concept, design, data analysis, literature search, manuscript editing, and manuscript review. M.J. contributed to data collection, data analysis, literature search, manuscript editing, and manuscript review. S.K.B. contributed to data analysis, literature search, manuscript editing, and manuscript review. S.P. contributed to literature search, manuscript editing, and manuscript review. N.D. contributed to literature search, manuscript editing, and manuscript review. A.P. contributed to literature search, manuscript editing, and manuscript review. S.M. contributed to literature search, manuscript editing, and manuscript review.

Funding

None.

Conflict of Interest

None declared.

References

1 Jung HS, Jee WH, McCauley TR, Ha KY, Choi KH. Discrimination of metastatic from acute osteoporotic compression spinal fractures with MR imaging. Radiographics 2003;23(01):179–187
2 Cicala D, Briganti F, Casale L, et al. Atraumatic vertebral compression fractures: differential diagnosis between benign osteoporotic and malignant fractures by MRI. Musculoskelet Surg 2013;97 (Suppl 2):S169–S179
3 Kaur A, Thukral CL, Khanna G, Singh P. Role of diffusion-weighted magnetic resonance imaging in the evaluation of vertebral bone marrow lesions. Pol J Radiol 2020;85:e215–e223
4 Karampinos DC, Ruschke S, Dieckmeyer M, et al. Quantitative MRI and spectroscopy of bone marrow. J Magn Reson Imaging 2018;47 (02):332–353
5 Maeda M, Sakuma H, Maier SE, Takeda K. Quantitative assessment of diffusion abnormalities in benign and malignant vertebral compression fractures by line scan diffusion-weighted imaging. Am J Roentgenol 2003;181(05):1203–1209
6 Jafarpour M, Faeghi F, Valizade A, Ghafouri M. The application of apparent diffusion coefficient and chemical shift images in differentiation of benign and malignant vertebral lesions. Int J Cancer Manag 2018;11(07):e66003
7 Baliyan V, Das CJ, Sharma R, Gupta AK. Diffusion weighted imaging: technique and applications. World J Radiol 2016;8 (09):785–798
8 Schmitz A, Risse JH, Textor J, et al. FDG-PET findings of vertebral compression fractures in osteoporosis: preliminary results. Osteoporos Int 2002;13(09):755–761
9 Yuh WT, Zachar CK, Barloon TJ, Sato Y, Sickels WJ, Hawes DR. Vertebral compression fractures: distinction between benign and malignant causes with MR imaging. Radiology 1989;172(01): 215–218
10 Baker LL, Goodman SB, Perkash I, Lane B, Enzmann DR. Benign versus pathologic compression fractures of vertebral bodies: assessment with conventional spin-echo, chemical-shift, and STIR MR imaging. Radiology 1990;174(02):495–502
11 Shih TT, Huang KM, Li YW. Solitary vertebral collapse: distinction between benign and malignant causes using MR patterns. J Magn Reson Imaging 1999;9(05):635–642
12 Eito K, Waka S, Naoko N, Makoto A, Atsuko H. Vertebral neoplastic compression fractures: assessment by dual-phase chemical shift imaging. J Magn Reson Imaging 2004;20(06):1020–1024
13 Drake-Pérez M, Boto J, Fitsiori A, Lovblad K, Vargas MI. Clinical applications of diffusion weighted imaging in neuroradiology. Insights Imaging 2018;9(04):535–547
14 Madhok R, Sachdeva P. Evaluation of apparent diffusion coefficient values in spinal tuberculosis by MRI. J Clin Diagn Res 2016; 10(08):TC19–TC23

15 Herneth AM, Philipp MO, Naude J, et al. Vertebral metastases: assessment with apparent diffusion coefficient. Radiology 2002; 225(03):889–894
16 Le Bihan DJ. Differentiation of benign versus pathologic compression fractures with diffusion-weighted MR imaging: a closer step toward the "holy grail" of tissue characterization? Radiology 1998;207(02):305–307
17 Nonomura Y, Yasumoto M, Yoshimura R, et al. Relationship between bone marrow cellularity and apparent diffusion coefficient. J Magn Reson Imaging 2001;13(05):757–760
18 Balliu E, Vilanova JC, Peláez I, et al. Diagnostic value of apparent diffusion coefficients to differentiate benign from malignant vertebral bone marrow lesions. Eur J Radiol 2009;69(03):560–566
19 Sheikh WA, Shaheen FA, Lone NA, Chhiber SS, Makhdoomi RH. Role of diffusion-weighted and chemical shift magnetic resonance imaging in differentiation of benign and malignant spinal fractures. Galician Med J 2020;27(03):E202037
20 Zhou XJ, Leeds NE, McKinnon GC, Kumar AJ. Characterization of benign and metastatic vertebral compression fractures with quantitative diffusion MR imaging. Am J Neuroradiol 2002;23 (01):165–170
21 Chan JHM, Peh WCG, Tsui EYK, et al. Acute vertebral body compression fractures: discrimination between benign and malignant causes using apparent diffusion coefficients. Br J Radiol 2002;75(891):207–214
22 Allam KE, Abd Elkhalek YI, Hassan HGEMA, Emara MAE. Diffusion-weighted magnetic resonance imaging in differentiation between different vertebral lesions using ADC mapping as a quantitative assessment tool. Egypt J Radiol Nucl Med 2022; 53:155
23 Turna O, Aybar M, Tuzcu G, Karagoz Y, Kesmezacar O, Turna I. Evaluation of vertebral bone marrow with diffusion weighted MRI and ADC measurements. Istanb Med J. 2014;15:116–121
24 Lavdas I, Rockall AG, Castelli F, et al. Apparent diffusion coefficient of normal abdominal organs and bone marrow from whole-body DWI at 1.5 T: the effect of sex and age. Am J Roentgenol 2015;205 (02):242–250
25 Aoki T, Yamaguchi S, Kinoshita S, Hayashida Y, Korogi Y. Quantification of bone marrow fat content using iterative decomposition of water and fat with echo asymmetry and least-squares estimation (IDEAL): reproducibility, site variation and correlation with age and menopause. Br J Radiol 2016;89(1065):20150538
26 Yoo HJ, Hong SH, Kim DH, et al. Measurement of fat content in vertebral marrow using a modified Dixon sequence to differentiate benign from malignant processes. J Magn Reson Imaging 2017; 45(05):1534–1544
27 Kim DH, Yoo HJ, Hong SH, Choi JY, Chae HD, Chung BM. Differentiation of acute osteoporotic and malignant vertebral fractures by quantification of fat fraction with a Dixon MRI sequence. Am J Roentgenol 2017;209(06):1331–1339
28 Fanucci E, Manenti G, Masala S, et al. Multiparameter characterisation of vertebral osteoporosis with 3-T MR. Radiol Med (Torino) 2007;112(02):208–223
29 Chang R, Ma X, Jiang Y, et al. Percentage fat fraction in magnetic resonance imaging: upgrading the osteoporosis-detecting parameter. BMC Med Imaging 2020;20(01):30

